Modelling and region stability analysis of wind turbines with battery energy storage system based on switched system with multi-equilibriums

Article (Accepted Version)

Modelling and Region Stability Analysis of Wind Turbines with Battery Energy Storage System based on Switched System with Multi-equilibriums

Xiaokun Dai[a] , Yang Song[a,b,*] and Taicheng Yang[c]

[a]Department of Automation, School of Mechatronic Engineering and Automation, Shanghai University, Shanghai 200444, China

[b]Shanghai Key Laboratory of Power Station Automation Technology, Shanghai 200444, China

[c]Department of Engineering and Design, University of Sussex, Brighton, BN1 9QT, UK

Abstract. This paper deals with the modelling and control for wind turbine combined with a battery energy storage system (WT/BESS). A PI controller of pitch angle is applied to adjust the output power of WT, and a method for battery scheduling is presented for maintaining the state of charging (SOC) of BESS. When the battery level is below the lower limit, we increase the expected output power of wind turbine through raising the operation point to charge the battery. Considering the effect of charging/discharging, a switched linear system model with two equilibriums is presented firstly for such WT/BESS system. The region stability is analyzed and an approach for estimating the corresponding stable region is also given. The effectiveness of the proposed results is demonstrated by a numerical example.

Keywords. Wind turbine, Rechargeable battery, Battery scheduling, Multiple equilibriums, Region stability

1 Introduction

With the increasing concerns on environment protection and emission reduction, wind energy, which is sustainable and clean, is nowadays exploited more extensively. In 2017, the newly installed capacity of wind power worldwide exceeds 50GW with a cumulative capacity of 539.6GW. However, the features of volatility and intermittency of wind bring challenges on harnessing wind energy as well as the technique of turbine access to power grid (Beik O et al., 2017; Wang Q et al., 2017; Li D et al., 2017; Yan H et al. 2017; Borges et al., 2017; Yin M et al., 2016).

The objects of the wind turbine control could be diverse for different cases. For example, when the wind speed is comparatively low, the control object is to capture the wind energy maximally by adjusting the rotor speed. By maximizing the power coefficient, an adaptive robust control scheme is proposed for maximum power capture in (Beltran et al., 2009; Zhao H et al., 2017). Sliding mode control (Beltran et al., 2009) as well as model predictive control (MPC) (Zhao H et al., 2017) has also been presented to track the maximum power point.

However, when wind speed is high and exceeds the demands of the connected power grid, the object of control in this case is changed to limit the output power of turbine by controlling the pitch angle (Johnson et al., 2011; Hwas et al., 2012; Chowdhury et al., 2012; Yilmaz A S et al. 2009; Lin Z et al., 2018; El-Tous,, 2008; Senjyu T, 2006; Matsuzaka, 1997). In practical engineering, pitch angle is often controlled by proportional-integral (PI) strategy (Johnson et al., 2011; Hwas et al., 2012). To improve the adaptiveness and the rapidness of the system, some intelligent methods such as fuzzy control

(Chowdhury et al., 2012) and neuro-network (Yilmaz A S et al. 2009) are applied to pitch angle control. Furthermore, considering the variation of wind speed, the dynamics of wind turbine is modelled as Markovian linear jump system and the stochastic stability of the WT system is investigated (Lin Z et al., 2018).

Aforementioned approaches of control can alleviate the output power fluctuation of WT to some extent. However, when the variation and the intermittency of wind energy is too excessively, it is not enough to smooth the power of WT purely by the control strategies. In this case, to compensate the power fluctuation of WT, an effective approach is to combine the wind turbine with a battery energy storage system (BESS) (Zhao T et al., 2017; Muhando et al., 2011; Meghni B et al., 2017). This BESS system can not only provide power to grid temporarily when the wind is too weak, it also absorbs the surplus output power of turbine for the case of high wind speed. In recent years, BESS systems have been applied extensively for wind turbine when connected to the grid. Since the battery and its maintenance take a large proportion in the total cost of WT/BESS system, some new topics of research are proposed, e.g. the minimum capacity of the BESS for wind farm (Howlader A M et al., 2015; Zhu W et al., 2013; Carpentiero V et al., 2012), the energy management strategy for extending the life span of battery, and etc. One of the difficulties for such problems is that the intermittency characteristics of wind should be taken into account.

In (Ma Z et al., 2015; Zhang L et al., 2010), some SOC regulate strategies of the battery are proposed by using a prediction model for wind speed changes. It should be noted that the wind turbine will increase (or decrease) the power output to the BESS when the battery is in charging (or discharging). This implies that, even if the wind speed remains constant, the operation points of the WT/BESS will change depending on the battery status of charging/discharging. From the perspective of switched systems, such WT/BESS can be described as a switched system with multiple equilibriums (SSME), where the two equilibriums in this paper are corresponding to the two different operation points of WT. The switching in the WT/BESS relies on the initial SOC and the energy regulation strategies of the BESS. It is well known that for a stable switched system with single equilibrium (i.e. the equilibriums of each subsystem are identical), the trajectory of the system will approach to the certain point equilibrium under appropriate switching sequences. Many contributions have reported on the stability of the switched system with single equilibrium for both arbitrary and time-dependent switching (Xiang W et al., 2018). However, for the system of SSME, the state trajectory cannot converge to a certain points but run reciprocally among the different equilibriums. Thus the notion of asymptotic stability is not suitable for the system of SSME. Region stability is defined for SSME system and a method for estimating the stable region is also proposed in (Guo R et al., 2017).

By means of the theoretic results of SSME, this paper deals with the modelling and the control of the WT/BESS which provides steady power to the grid. To the best knowledge of the authors, there is no similar result reported on the studies of WT/BESS from the point of SSME. The contributions of this paper are threefold: 1) a SSME model is established for WT/BESS; 2) region stability is studied and a stable region is given; 3) a PI controller is designed for pitch angle control with the region stability are guaranteed.

This paper is structured as follows: Section 2 describes the dynamics of WT as well as the proposed SOC scheduling method of BESS. In Section 3, the WT/BESS is modeled as a SSME and the region stability is investigated. A controller design method is also given in this section. Finally, a numerical example is given in Section 4. Section 5 concludes this paper.

Notation

$\mathbb{R}$ and $\mathbb{C}$ denote the sets of real and complex numbers, and $\mathbb{R}^n$ is the n-dimensional Euclidean space respectively. $\lambda_{max}(\cdot)/\lambda_{min}(\cdot)$ denote the maximum/ minimum eigenvalues of matrices, respectively. $\|\bullet\|$ means the European norm of vector in $\mathbb{R}^n$, i.e. $\|x\| = \sqrt{(|x_1|^2 + |x_2|^2 + \cdots + |x_n|^2)}$.

2 WT/BESS Model

The structure diagram of a WT/BESS system is shown in Figure 1. The instantaneous power generated by the wind turbine P_g is generally fluctuant due to the variation of wind speed. To smooth the power supplied to grid, i.e. P_c in Figure 1, a battery energy storage system is integrated into the wind turbine system, the output power ΔP_b of such battery system is used to compensate P_c. And P_g^* is the expected output power of wind turbine. To extend the battery lifespan, when the battery level is below the lower limit, we increase the expected output power P_g^* of wind turbine through raising the operation point to charge the battery. When the battery needs to be charged, we divide the charge and discharge power of battery into two parts equally. One part is to charge the battery at a fixed power P_{charge}, and the other part still uses ΔP_b to smooth the output power of the WT/BESS system to the grid.

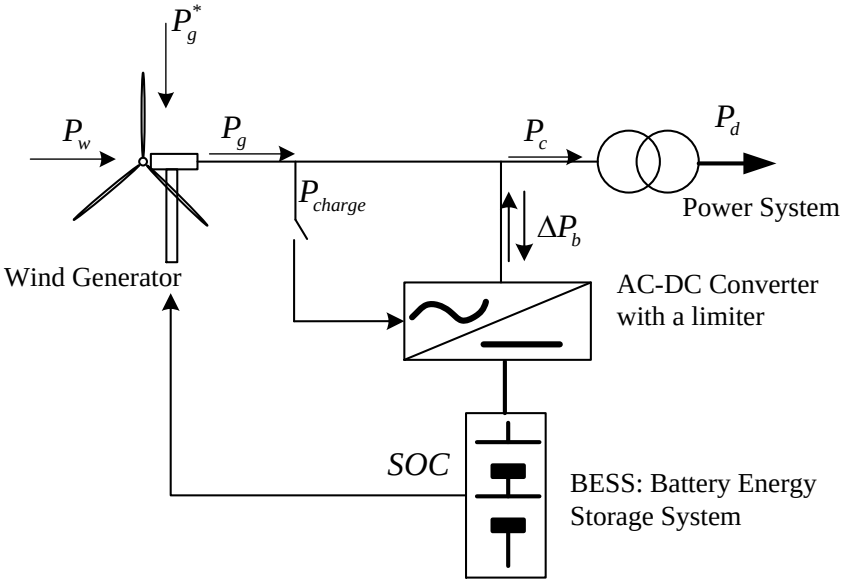

Figure 1. Wind turbine system with BESS.

2.1 WT Model

In general, the instantaneous power P_w captured by a wind turbine from wind energy can be expressed as

$$P_w = \frac{1}{2}\rho\pi R^2 v^3 C_p(\lambda, \beta), \quad (1)$$

where ρ is the air density, R is the rotor radius, v is the instantaneous wind speed, β is the turbine's blade pitch angle, $\beta \in [0^\circ, 90^\circ]$, λ is called as tip-speed ratio which is defined by $\lambda = \omega R / v$, i.e. the ratio of the tangential speed of the blade tip to the wind speed, ω is the rotor angular velocity. C_p is the power coefficient which is given as [11]:

$$C_P = 0.4654\left(\frac{116}{\lambda'} - 0.4\beta - 5\right)e^{\frac{-20.24}{\lambda'}} \tag{2}$$

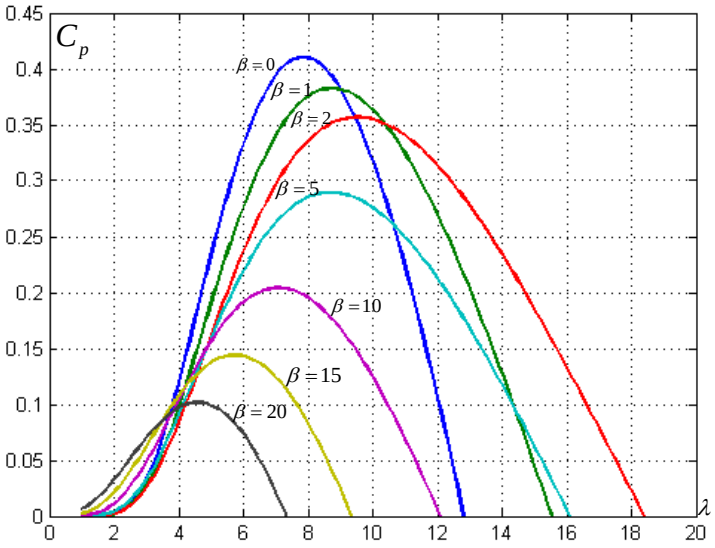

Figure 2. $C_p - \lambda$ curves for different pitch angle.

where $\frac{1}{\lambda'} = \frac{1}{\lambda + 0.08\beta} - \frac{0.035}{\beta^3 + 1}$. Figure 2 illustrates $C_p - \lambda$ characteristic curves for different pitch angles.

To make the instantaneous power of the turbine P_w equals a constant demand, the expected wind speed v_d and the corresponding rotor speed ω_s can be obtained by Eq. (1) and the power coefficient formula (2). In this paper, the particular rotor speed ω_s is called the operation point of the wind turbine.

The power curve of turbine is given in Figure 3, where operation of the turbine is divided by three regions. In Region 1, the wind turbine will not run due to the wind speed is lower than the minimum required wind speed v_{in}. In Region 2 in which the wind speed is in between v_{in} and v_d, the output power of the wind turbine cannot reach the demand power. In this case the BESS could be utilized to supplement extra energy to satisfy the demand of power grid. In Region 3, the wind energy will exceed the demand of power grid. Thus, in this case the output power of wind turbine needs to be limited by adjusting the pitch angle β and by charging the BESS jointly.

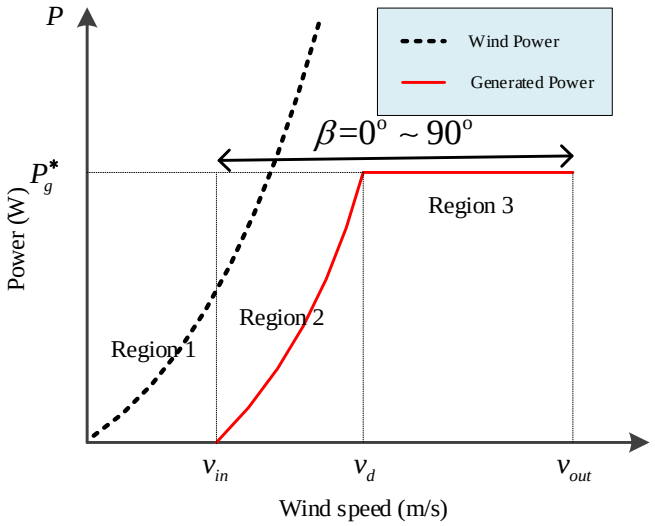

Figure 3. Output power curves of wind turbine.

The dynamic model of the wind turbine can be expressed as

$$\dot{\omega} = \frac{1}{J}(\tau_{aero} - \tau_d), \tag{3}$$

$$P_g = \tau_d \omega. \tag{4}$$

where J is the rotational inertia of the turbine, the aerodynamic torque τ_{aero} is given by

$$\tau_{aero} = \frac{1}{2}\rho\pi R^2 v^3 \frac{C_p(\lambda, \beta)}{\omega}. \tag{5}$$

The load torque of the wind turbine τ_d is generally set as

$$\tau_d = \frac{P_g^*}{\omega_s}. \tag{6}$$

where P_g^* is the expected output power due to the requirement of grid.

To prevent undesirable over-speed faults, a PI controller is applied to implement for controlling the pitch angle,

$$\beta(t) - \beta_s = K_P \omega_e(t) + K_I \int_0^t \omega_e(\tau) d\tau, \tag{7}$$

where $\omega_e = \omega - \omega_s$ and β_s is the expected pitch angle corresponding to the average speed of wind. Therefore

$$\dot{\beta} = K_P \dot{\omega} + K_I(\omega - \omega_s). \tag{8}$$

To analyze the stability for wind turbine, the method of linearization as follows is often used (Palejiya et al., 2013, Lin Z et al., 2018). Apply the Taylor expansion around the point (ω_s, β_s, v_s) at the average speed of wind for (3) and (8), which yields

$$\dot{\omega} \approx \frac{1}{J}\left(\frac{\partial \tau_{aero}}{\partial \omega}\Big|_{\omega=\omega_s} (\omega - \omega_s) + \frac{\partial \tau_{aero}}{\partial \beta}\Big|_{\beta=\beta_s} (\beta - \beta_s) + \frac{\partial \tau_{aero}}{\partial v}\Big|_{v=v_s} (v - v_s) \right). \tag{9}$$

$$\dot{\beta} \approx \frac{K_P}{J}\left(\frac{\partial \tau_{aero}}{\partial \beta}\Big|_{\beta=\beta_s}(\beta-\beta_s)+\frac{\partial \tau_{aero}}{\partial v}\Big|_{v=v_s}(v-v_s)\right)+\left(\frac{K_P}{J}\frac{\partial \tau_{aero}}{\partial \omega}\Big|_{\omega=\omega_s}+K_I\right)(\omega-\omega_s). \quad (10)$$

2.2 BESS Model

According to the battery access method in (Howlader A M et al., 2015), BESS model is shown in Figure 4. The smooth power ΔP_b of the battery is related to three variables: the combined power from the WT/ BESS to the grid P_c, the expected power P_c^* and the SOC of the battery. Figure 5 in below presents the control structure of the BESS for maintaining the storage energy of the battery in a proper range. When the SOC of the battery is below the lower limit, the wind turbine will supply extra power to charge the BESS, thus the operation point of the wind turbine will shift in this case.

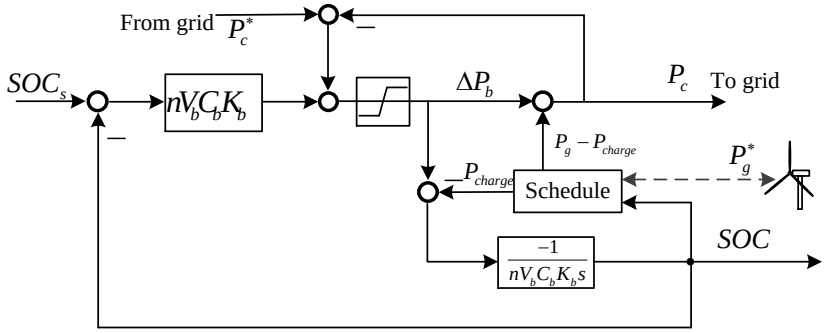

Figure 4. Control system of BESS.

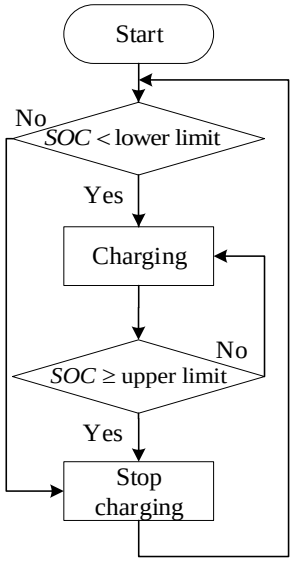

Figure 5. The schedule of battery charging.

When the battery is in charge, the dynamics of the battery system

$$\Delta P_b = nV_bC_bK_b\left(SOC - SOC_s\right) + P_c^* - P_c(t)$$

where $P_c(t) = \Delta P_b + P_g(t) - P_{charge}$ and $P_c^* = P_g^* - P_{charge}$, thus

$$\frac{d}{dt}SOC(t) = \frac{P_c(t) - P_c^*}{nV_bC_b} + \frac{P_{charge}}{nV_bC_b} + K_b\left(SOC - SOC_s\right)$$

$$= \frac{\tau_d}{2nV_bC_b}(\omega - \omega_s) + 0.5K_b(SOC - SOC_1) \quad (11)$$

where $SOC_1 = SOC_s - \frac{2P_{charge}}{nK_bV_bC_b}$, n is the number of batteries, V_b is the terminal voltage of battery, and C_b is the nominal energy capacity of battery bank in kAh.

When the battery is not in charge, i.e. $P_{charge}=0$, thus (11) is degenerate into

$$\frac{d}{dt}SOC(t) = \frac{\tau_d}{2nV_bC_b}(\omega - \omega_s) + 0.5K_b(SOC - SOC_2) \quad (12)$$

where $SOC_2 = SOC_s$.

3 SSME Model and Region Stability for WT/BESS

For a WT/BESS, when the battery needs not charge, the output power of wind turbine is generally set to be the demand of power grid, i.e. $P_g^* = P_d$. When the SOC of battery is too low, the output power of wind turbine will not only meet the demand of power grid, but also need to provide additional power P_{charge} for charging the batter system, i.e. $P_g^* = P_d + P_{charge}$. Hence, the operation point of wind turbine, which is the junction point of region2 and region3, will shift because the demand power is changed. Thus the rotor speed ω_s at the operation point will be raised from ω_2 to ω_1. And due to that both rotor speed ω_s and demand power at average speed of wind is different when charging/discharging, the expected pitch angle β_s corresponding to average speed of wind will also shift from β_1 to β_2. Therefore, the model of wind turbine is linearized at (ω_1, β_1) and (ω_2, β_2) respectively by distinguishing the two cases of charging and discharging, as shown in Figure 6.

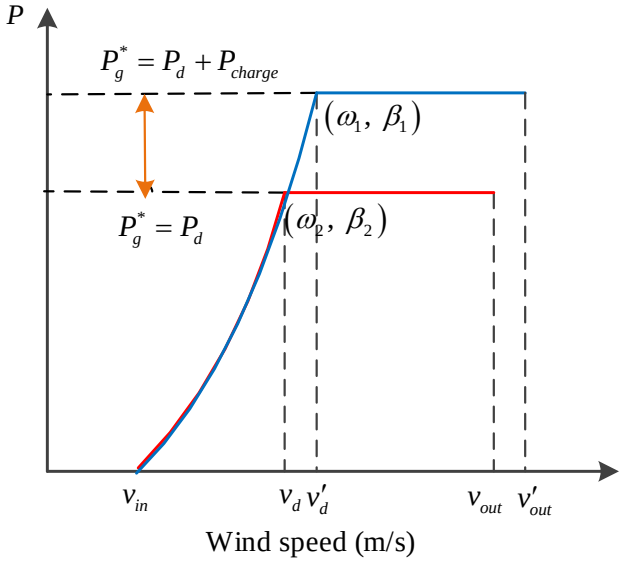

Figure 6. Operation points of WT/BESS.

Select a set of PI controller parameters K_P^i, K_I^i for each subsystem in this paper. After linearization on the two equilibriums and notice (9) – (12), a model of switched system with multiple equilibriums (SSME) is presented as below,

$$\begin{bmatrix} \dot{x} \\ \dot{SOC} \end{bmatrix} = \begin{bmatrix} A_i + BK_i & 0 \\ C_i & 0.5K_b \end{bmatrix} \left(\begin{bmatrix} x \\ SOC \end{bmatrix} - \begin{bmatrix} x_i^e \\ SOC_i^e \end{bmatrix} \right) + \begin{bmatrix} D_i \\ 0 \end{bmatrix} (v - v_i). \tag{13}$$

where $x = \begin{bmatrix} \beta \\ \omega \end{bmatrix}$, $x_i^e = \begin{bmatrix} \beta_i \\ \omega_i \end{bmatrix}$, $A_i = \frac{1}{J} \begin{bmatrix} 0 & 0 \\ f\big|_{\beta_i} & f\big|_{\omega_i} \end{bmatrix}$, $f\big|_{\beta_i} = \frac{\partial \tau_{aero}}{\partial \beta}\Big|_{\beta=\beta_i}$, $f\big|_{\omega_i} = \frac{\partial \tau_{aero}}{\partial \omega}\Big|_{\omega=\omega_i}$,

$f\big|_{v_i} = \frac{\partial \tau_{aero}}{\partial v}\Big|_{v=v_i}$ and $B = \begin{bmatrix} 1 \\ 0 \end{bmatrix}$, $K_i = \begin{bmatrix} \frac{K_P^i}{J} f\big|_{\beta_i} & \frac{K_P^i}{J} f\big|_{\omega_i} + K_I^i \end{bmatrix}$, $C_i = \begin{bmatrix} 0 & \frac{\tau_{d_i}}{2nV_bC_b} \end{bmatrix}$, $D_i = \frac{1}{J} \begin{bmatrix} K_P^i f\big|_{v_i} \\ f\big|_{v_i} \end{bmatrix}$,

$\tau_{d_1} = \left(P_d + P_{charge}\right)/\omega_1$, $\tau_{d_2} = P_d/\omega_2$, $SOC_1^e = SOC_s - \frac{2P_{charge}}{nK_bV_bC_b}$, $SOC_2^e = SOC_s$.

It can be seen from (13) that the two subsystem equations of wind turbine have no direct relationship with the SOC of battery. However, the variation of the latter could affect the switching of operation point of wind turbine. At the same time, the change of wind speed will also cause such equilibrium switching. Since the change of wind speed is generally difficult to predict, it is hard to describe the law of the operation point switching. Therefore, the switching process of operation point of turbine in this paper is regarded to be arbitrary when stability analysis. In the following, the region stability of a switched linear system with two equilibriums (14) as below is investigated.

$$\dot{x} = \bar{A}_{\sigma(t)} \left(x - x_{\sigma(t)}^e \right), \tag{14}$$

where the switching law $\sigma(t) \in \{1, 2\}$, $\bar{A}_i = A_i + BK_i$.

Different from the single equilibrium system, the trajectory of a SSME cannot converge to a certain point, which implies that it is impossible to be asymptotic stable for a SSME as long as the switching of subsystem does not terminate. In (Guo R et al., 2017), the concept of region stability is proposed for SSME, the definition of which is given as below. In brief, a SSME is region stable if the trajectory of the system under arbitrary switching sequence will converge to a set called stable region. Clearly, the stable region contains all the equilibrium points of the SSME. The studies on the region stability conditions and the methods for estimating the stable region are still in progress.

Definition 3.1 (Region Stability) (Guo R, 2017) For $\forall x_0 \in \mathbb{R}^n$ and an arbitrary switching path $\sigma(t)$, denote by $x_{\sigma(t)}(t; t_0, x_0)$ the trajectory of the switched system (14) starting from x_0 . Letting $\Omega_w \subset \mathbb{R}^n$ be a domain containing all the equilibrium of the subsystems, if for $\forall x \in x_{\sigma(t)}(t; t_0, x_0)$, $\lim_{t\to\infty} dis(x_{\sigma(t)}(t, t_0, x_0), \Omega_w) = 0$, then the switched system (14) is called region stable on Ω_w and Ω_w is said a Stable Rough Region (SRR) under arbitrary switching paths, where $dis(x_{\sigma(t)}(t, t_0, x_0), \Omega_w) := \inf\left\{ |x - y| : \forall y \in \Omega_w \right\}$. The minimum among all the stable rough regions, that is, $\bigcap_w \Omega_w$ is called the stable region under arbitrary switching paths.

Based on the common Lyapunov function method, the following sufficient conditions of region stability and the estimation of the corresponding stable region is given for SSME (14).

Theorem 3.1 Consider a SSME (14) , if there exit a positive definite matrix X and matrix W_i such that $\bar{A}_i X + BW_i + (\bar{A}_i X + BW_i)^T < 0, i = 1,2$, then system (14) is region stable under arbitrary switching paths, and the feedback control law is $K_i = W_i X^{-1}$, the corresponding stable region can be given as

$$\Omega = \left\{ x \in \mathbb{R}^n : (x - \bar{x}) X^{-1} (x - \bar{x}) \le C \right\}, \tag{15}$$

where $\bar{x} = (x_1^e + x_2^e)/2$, and

$$C = \lambda_{max}(X^{-1}) \left(\max_{i \in \{1,2\}} \|\eta_i - \bar{x}\| + \max_{i \in \{1,2\}} \|\xi_i\| \right)^2, \tag{16}$$

$$\xi_i = (\bar{A}_i + BK_i) X^{-1} (x_i^e - \bar{x}) / \lambda_{min}(Q_i), \tag{17}$$

$$\eta_i = \xi_i + x_i^e, Q_i = -(\bar{A}_i + BK_i)^T X^{-1} + X^{-1}(\bar{A}_i + BK_i), i = 1,2. \tag{18}$$

Proof According Corollary 1 in (Guo R et al., 2017), if the special system (19) which is ordinary switched system of SSME (14) shares a CLF

$$\dot{x} = \bar{A}_i x, \quad x \in \mathbb{R}^n, \quad i = 1,2. \tag{19}$$

Hence, if there exists a positive definite matrix P , that

$$(A_i + BK_i)^T P + P(A_i + BK_i) < 0, \tag{20}$$

then the system is region stable under arbitrary switching paths. The corresponding stable region is

$$\Omega = \left\{ x \in \mathbb{R}^n : (x - \bar{x}) P (x - \bar{x}) \le C \right\}, \tag{21}$$

Left and right multiplication matrix P^{-1} (19) and define $X = P^{-1}$ and $W_i = K_i X$, then (16) - (18) are obtained. This completes the proof. □

To reduce the oscillation of trajectory between different operation points, a smaller stable region Ω could be obtained if the feedback laws K_i are selected appropriately. The procedure of the controller design for the WT/BESS system is given as follows:

Controller design procedures:

Step 1: Calculate two equilibriums x_1^e, x_2^e at average speed of wind. According to the maximum power coefficient, the expected wind speeds, i.e. v_1, v_2 on the two operation points can be calculated to make instantaneous power of the turbine P_w equals a constant demand. Hence, the corresponding rotor speed ω_1, ω_2 and expected β_1, β_2 at average speed of wind can be obtained respectively by Eq. (1) and the power coefficient formula (2).

Step 2: Linearize the WT/BESS model on the two equilibriums respectively and obtain linear SSME (9) and (10).

Step 3: For theorem 3.1, the positive definite matrix X can be solved by the LMI toolbox in MATLAB. To make the stable region smaller, calculate matrix X and matrix W_i by itineration. Then according to theorem 3.1, the parameters of K_P^1, K_I^1 and K_P^2, K_I^2 and the stable region Ω are obtained.

4 Numerical example

Considering a practical WT/BESS given in (Palejiya et al., 2013), where the rotor radius $R = 9m$, the rotor inertia $J = 26000kg \cdot m^2$, $C_{pmax} = 0.4101$, the demand power of grid $P_d = 40\text{kW}$, and the charging power of battery bank $P_{charge} = 20\text{kW}$, the number of batteries $n = 10$ and $K_b = -0.02$, the terminal voltage and the nominal energy capacity of a single battery are V_b=48V, $C_b = 480\text{kAh}$ respectively.

Assume the average wind speed is 12m/s, and by following the design procedure presented in Section 3, the PI controller and the corresponding stable region are obtained.

Step 1: According to the three parameters P_d, P_{charge}, C_{pmax}, the wind speeds in two operation points can be obtained, $v_1 = 9.3m/s$, $v_2 = 8.4m/s$. Thus, x_1^e, x_2^e in (14) are

$$\begin{aligned} x_1^e &: \beta = 7.55^\circ, \omega = 8.146rad/s; \\ x_2^e &: \beta = 15.25^\circ, \omega = 7.326rad/s. \end{aligned}$$

Step 2: Linearize the WT/BESS model on the two equilibriums and then we get $f|_{\beta_1} = -0.0084$, $f|_{\omega_1} = 0.0015$, $f|_{\beta_2} = -0.0131$, $f|_{\omega_2} = -0.0236$ .The state matrix of the two subsystems in (14) is

$$A_1 = \begin{bmatrix} 0 & 0 \\ -0.0084 & 0.0015 \end{bmatrix}, \ A_2 = \begin{bmatrix} 0 & 0 \\ -0.0131 & -0.0236 \end{bmatrix}.$$

Step 3: By Theorem 3.1, it can be obtained that

$$X^{-1} = \begin{bmatrix} 4543.9 & 46.8 \\ 46.8 & 23.1 \end{bmatrix}, W_1 = \begin{bmatrix} -3181600 & -33200 \end{bmatrix}, W_2 = \begin{bmatrix} -908610 & -9270 \end{bmatrix}.$$

Thus

$$K_P^1 = -700, K_I^1 = -18.5 \text{ and } K_P^2 = -200, \ K_I^2 = -3.5. \tag{22}$$

And the corresponding stable region is

$$\Omega = \left\{ x \in \mathbb{R}^n : (x - \bar{x}) X^{-1} (x - \bar{x}) \le 1.2368 \right\}.$$

Then, the closed-loop state matrices of the subsystems

$$\bar{A}_1 = \begin{bmatrix} -5.9125 & 19.5701 \\ -0.0084 & 0.0015 \end{bmatrix}, \ \bar{A}_2 = \begin{bmatrix} -2.6139 & -1.2217 \\ -0.0131 & -0.0236 \end{bmatrix}. \tag{23}$$

Under aforementioned conditions, the trajectories of the SSME for wind turbine are shown in Figure 7. For comparison, Figure 7 (a) and Figure 7 (b) shows the state change trajectories at wind speeds of 12 m/s with two different PI controllers respectively, where the controller parameters used in Figure 7 (a) are chosen as (22), and the other PI controller parameters are $K_P^1 = -20$, $K_I^1 = -1$ and $K_P^2 = -18$, $K_I^2 = -2$. One can see that, although both the two controllers can guarantee the WT/BESS is region stable, the former PI controller, which is obtained by the proposed procedure in Section 3, has smaller stable region than the latter.

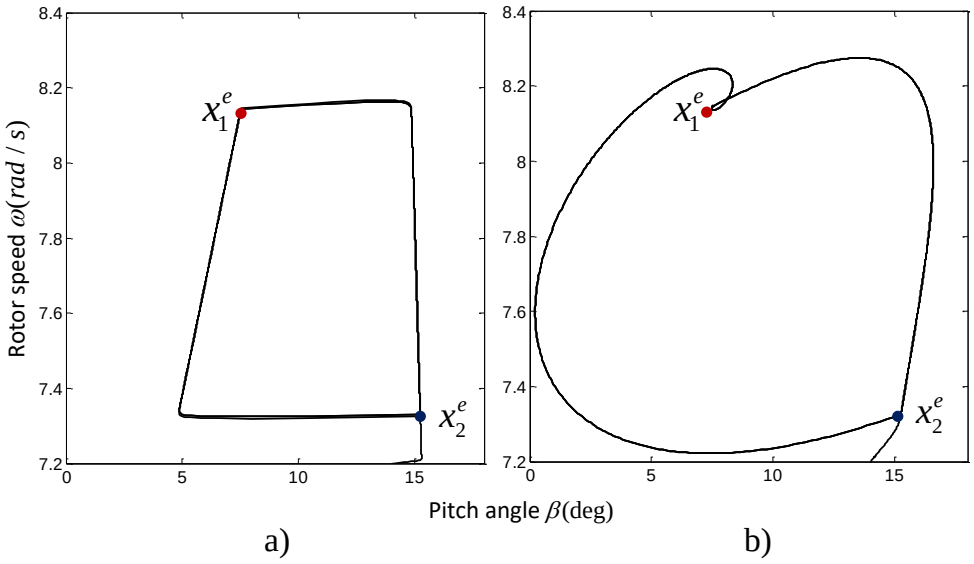

Figure 7. The trajectories of turbine: a) PI controllers chosen as (22), b) PI controllers chosen as $K_P^1 = -20$, $K_I^1 = -1$, $K_P^2 = -18$, $K_I^2 = -2$.

When the wind speed is as in Figure 8, Figure 9 gives the response of the WT/BESS. In detail, Fig. 9(a) is the switching of the operating point of the wind turbine, which is synchronous with the switching between the modes of charging and discharging of the battery. Figure 9(b) shows the plot of pitch angle. Fig. 9(c) shows the plots of wind turbine rotor speed, which demonstrates the proposed results (the solid red line) is better than other results (the dotted black line) (Palejiya et al., 2013) which is based on the single equilibrium analysis (Palejiya et al., 2013). Finally, it can be seen from Figures 10 and 11 that the proposed schedule method of battery energy can keep the SOC with the expected range and smooth the output power of WT/BESS effectively.

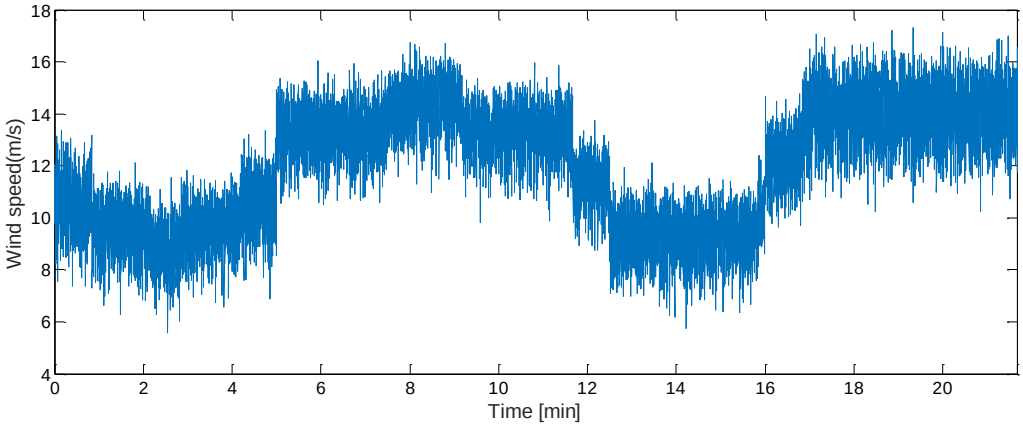

Figure 8. The curve of wind speed.

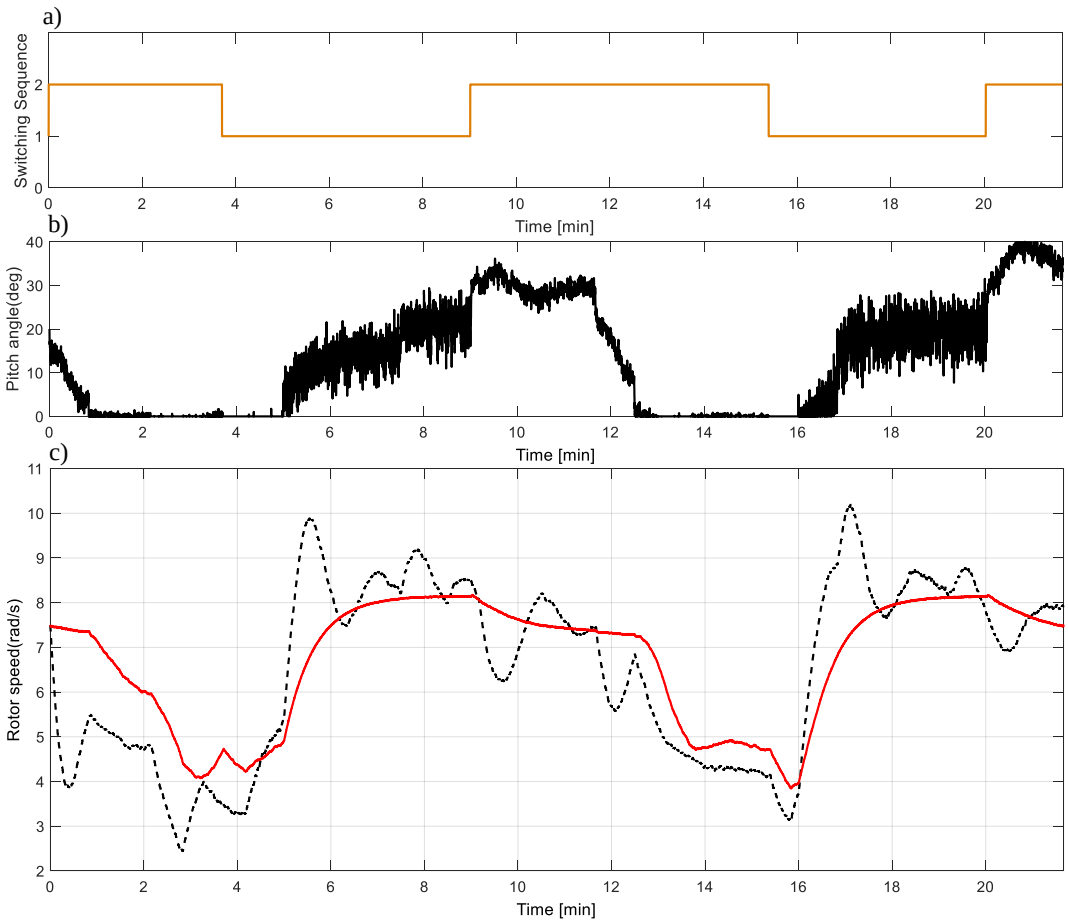

Figure 9. Simulation results: a) the switching path of the SSME of the WT, b) Blade pitch angle, c) rotor speed of the WT.

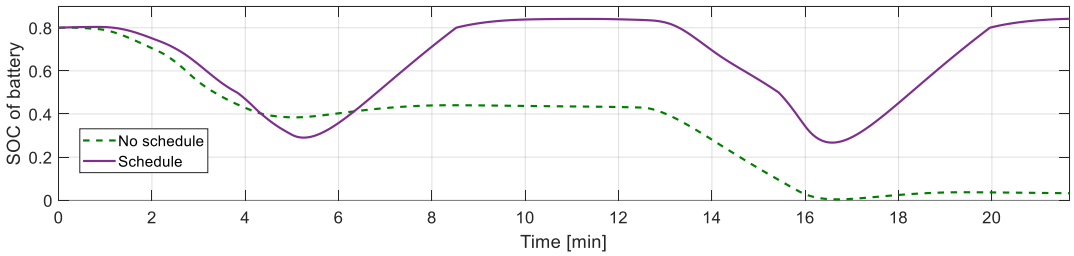

Figure 10. The SOC of the battery.

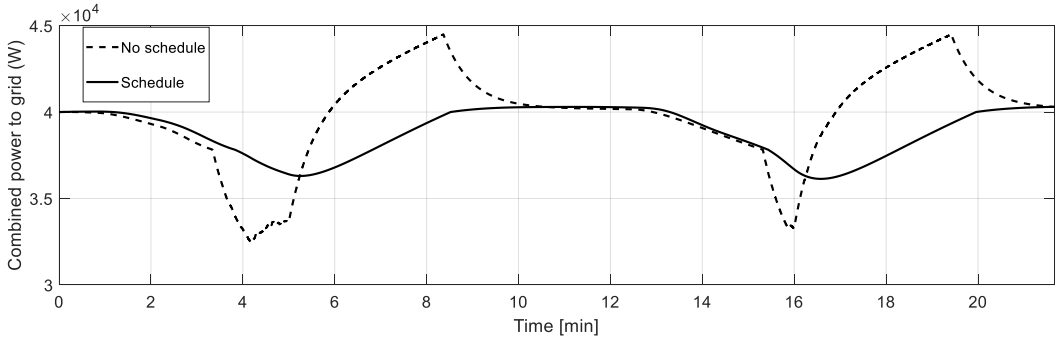

Figure 11. The combined output power P_c supplied to grid.

5 Conclusion

This paper studies the modelling and control of wind turbine with battery energy storage system. Noticing the switching of the operating point of the wind turbine during battery charging/discharging in a WT/BESS system, this paper proposed a model of switched linear system with multiple equilibriums accordingly. The region stability is analyzed and an approach for estimating the corresponding stable region is also given. Combined with PI control and battery's schedule, this paper gives the design procedures of controller parameters. In the further study we will investigate the region stability of WT/BESS under wind fluctuations.

Acknowledgments

This work was supported by the National Natural Science Funds of China (61573237, 61633016, and 61773251) and 111 Project (D18003).

References

Beik O, and Schofield N (2018) High-Voltage Hybrid Generator and Conversion System for Wind Turbine Applications. *IEEE Transactions on Industrial Electronics* 65(4): 3220-3229.

Beltran B, Ahmed-Ali T, and Benbouzid M. E. H. (2009) High-order sliding-mode control of variable-speed wind turbines. *IEEE Transactions on Industrial Electronics* 56(9): 3314-3321.

Billy P, Muhando E, Senjyu T, Uehara A and Funabashi T (2011) Gain-scheduled H∞ control for WECS via LMI techniques and parametrically dependent feedback. Part I: Model development fundamentals. *IEEE Transactions on Industrial Electronics* 58(1): 48-56.

Borges C. L., Aredes M. A., and Singh C (2017) A probabilistic approach to the evaluation of energy availability of fixed and variable speed wind turbines. In: *IEEE Pes Innovative Smart Grid Technologies Conference Europe*, Torino, Italy, September, pp. 1-6.

Carpentiero V, Langella R, and Testa A (2012) Hybrid wind-diesel stand-alone system sizing accounting for component expected life and fuel price uncertainty. *Electric Power Systems Research* 88(7): 69-77.

Chowdhury M. A., Hosseinzadeh N and Shen W (2012) Smoothing wind power fluctuations by fuzzy logic pitch angle controller. *Renewable Energy* 38(1): 224–233.

El-Tous, Y. (2008) Pitch angle control of variable speed wind turbine. *American Journal of Engineering and Applied Sciences* 1(2): 118-120.

Guo R, and Wang Y (2017) Region stability analysis for switched linear systems with multiple equilibria. *International Journal of Control Automation & Systems* 15(2): 567-574.

Howlader A M, Matayoshi H and Senjyu T (2015) A Robust H∞ Controller Based Gain-scheduled Approach for the Power Smoothing of Wind Turbine Generator with a Battery Energy Storage System. *Electric Machines & Power Systems* 43(19):2156-2167.

Hwas, Abdulhamed and R. Katebi (2012) Wind Turbine Control Using PI Pitch Angle Controller. *IFAC Proceedings Volumes* 45(3):241-246.

Johnson and L. P. K. (2011). Control of wind turbines. approaches, challenges, and recent developments. *IEEE Control systems magazine* 58(4): 44-62.

Li D, Li P, Cai W, Song Y and Chen H (2018) Adaptive Fault Tolerant Control of Wind Turbines with Guaranteed Transient Performance Considering Active Power Control of Wind Farms. *IEEE Transactions on Industrial Electronics* 65(4): 3275-3285.

Lin Z, Liu J, Wu Q and Niu Y (2018) Mixed H2/H∞ Pitch Control of Wind Turbine with a Markovian Jump Model. *International Journal of Control* 91(1):156-169.

Matsuzaka T and Tuchiya K (1997) Study on stabilization of a wind generator power fluctuation. *IEEJ Transactions on Power and Energy* 117(5): 625-633.

Ma Z and Chen D (2015) Optimal power dispatch and control of a wind turbine and battery hybrid system. In*: American Control Conference*, Chicago, IL, USA, July, pp. 3052-3057.

Meghni B, Dib D, Azar A T, Ghoudelbourk S and Saadoun A (2017) Robust Adaptive Supervisory Fractional Order Controller for Optimal Energy Management in Wind Turbine with Battery Storage. *Fractional Order Control and Synchronization of Chaotic Systems* pp.165-202.

Meghni B, Dib D and Azar A T (2017) A second-order sliding mode and fuzzy logic control to optimal energy management in wind turbine with battery storage. *Neural Computing and Applications* 28(6): 1417-1434.

Palejiya D, Hall J, Mecklenborg C and Chen D (2013) Stability of Wind Turbine Switching Control in an Integrated Wind Turbine and Rechargeable Battery System: A Common Quadratic Lyapunov Function. *Approach Journal of Dynamic Systems Measurement & Control* 135(2):44-45.

Senjyu T, Sakamoto R, Urasaki N, Funabashi T, Fujita H, and Sekine H (2006) Output power leveling of wind turbine generator for all operating regions by pitch angle control. *IEEE Transactions on Energy Conversion* 21(2): 467-475.

Wang Q and Niu S (2017) Design, Modeling and Control of a Novel Hybrid Excited Flux Bidirectional Modulated Generator Based Wind Power Generation System. *IEEE Transactions on Power Electronics* 33(4): 3086-3096.

Xiang W, Tran H D and Johnson T T (2018) Robust Exponential Stability and Disturbance Attenuation for Discrete-Time Switched Systems under Arbitrary Switching. *IEEE Transactions on Automatic Control* 63(5): 1450-1456.

Xiang W (2018) Parameter-memorized Lyapunov functions for discrete-time systems with time-varying parametric uncertainties. *Automatica* 87(1): 450-454.

Xiang W, Lam J, and Shen J (2017) Stability analysis and L1-gain characterization for switched positive systems under dwell-time constraint. *Automatica* 85(12): 1-8.

Yan H, Zhou X, Zhang H, Yang F and Wu Z (2017) A Novel Sliding Mode Estimation for Microgrid Control with Communication Time Delays. *IEEE Transactions on Smart Grid* DOI 10.1109/TSG.2017.2771493.

Yilmaz A S and Özer Z (2009) Pitch angle control in wind turbines above the rated wind speed by multi-layer perceptron and radial basis function neural networks. *Expert Systems with Applications* 36(6): 9767-9775.

Yin M, Xu Y, Shen C, Liu J, Dong Z and Zou Y (2016) Turbine Stability-Constrained Available Wind Power of Variable Speed Wind Turbines for Active Power Control. *IEEE Transactions on Power Systems* 32(3): 2487-2488.

Zhang L and Wirth A (2010) Wind energy management with battery storage. *Journal of the Operational Research Society* 61(10):1510-1522.

Zhao H, Wu Q, Guo Q, Sun H and Xue Y (2017) Distributed Model Predictive Control of a Wind Farm for Optimal Active Power Control Part I: Clustering-Based Wind Turbine Model Linearization. *IEEE Transactions on Sustainable Energy* 6(3):831-839.

Zhao T and Ding Z (2017) Cooperative Optimal Control of Battery Energy Storage System under Wind Uncertainties in a Microgrid. *IEEE Transactions on Power Systems* 33(2): 2292-2300.

Zhu W, Zhu Y, Davis Z and Tatarchuk B J (2013) Energy efficiencyand capacity renetation of Ni-MH batteries for storageapplications. *Applied Energy* 106: 307–313.